Partial-Boundary Element Method for Analysis of Striplines with Arbitrary Cross-Sectional Dielectric in Multi-layered Media

Kazuhiko Atsuki, *Member, IEEE*, and Keren Li, *Member, IEEE*

***Abstract*—A new method of analysis called the partial-boundary element method (p-BEM) is proposed for the analysis of striplines with arbitrary cross-sectional dielectric in multi-layered media. By using a Green's function that satisfies the boundary conditions of a relevant structure with multi-layered media and introducing a concept of the equivalent charge density, the p-BEM formulates a potential integral and boundary integral equations only on partial-boundaries such as the surface of the arbitrary cross-sectional dielectric. The number of the equations needed to be formulated is much less than in the conventional BEM. Numerical results of analysis are presented for two kinds of striplines: 1) with a rectangular dielectric ridge and 2) with an embedded rectangular dielectric in three-layered media.**

I. Introduction

THE increasing importance of miniature and integrated microwave circuits in the recent years has renewed interest on the microwave circuit designer in various microwave systems such as mobile communications, etc. To meet the strong demands of the low cost and high functions of microwave systems in commercial products, it has been proposed that integrated microwave circuits be monolithic (MMIC's) and multi-layered [1]. The MMIC's involve a number of active devices and passive components and are fabricated on a semiconductor wafer like GaAs. The advanced semiconductor processing techniques employed in the manufacture of the MMIC's allow microwave circuits to have a complicated cross-section of substrate and multi-layered media [1], [2], [12]. Fig. 1 shows a structure, based on a practical waveguide called Microslab™ and proposed for loss reduction of the microstrip lines, which consists of a conducting strip on a dielectric ridge placed on dielectric substrates [3]. Fig. 2 shows a microstrip line embedding a different dielectric material in the substrate under the conducting strip, the configuration of which is similar to the structure of the FET device. As illustrated, these structures consist of a rectangular cross-sectional dielectric in multi-layered media, and one conducting strip.

For design purposes, it is necessary to know how the characteristic impedance, propagating constant, and attenuation constant of these transmission lines depend on geometrical factors, on the properties of dielectric materials and conductors. For the analysis of these lines, however, several methods

Manuscript received December 14, 1993; revised September 26, 1994.

The authors are with the Department of Electronic Engineering, The University of Electro-Communications, Tokyo 182, Japan.

IEEE Log Number 9410341.

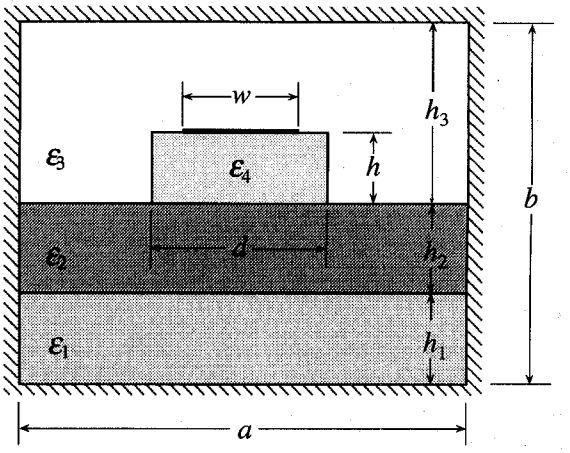

Fig. 1. Stripline with a rectangular dielectric ridge in three-layered media.

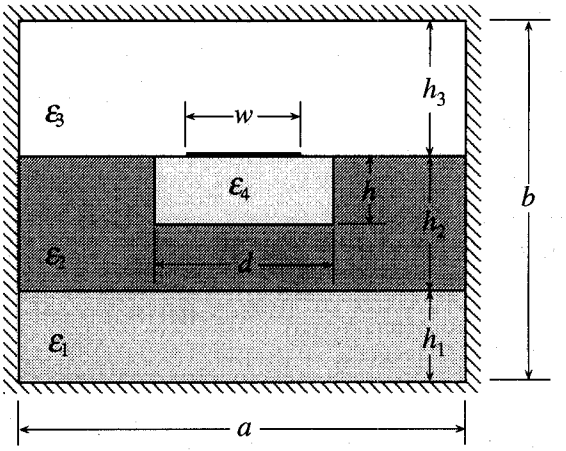

Fig. 2. Stripline with an embedded rectangular dielectric in three-layered media.

widely used in the analysis of microwave transmission lines, such as the conformal mapping technique, the spectral domain approach (SPA) [4] and the rectangular boundary division method [5], are difficult to apply because of the complicated cross-sections shown in Figs. 1 and 2. Two other widely used numerical analysis methods, namely, the finite element method (FEM) and the boundary element method (BEM) [6], [7], [11], [12], are applicable to the analysis of these lines. The FEM is easily applied to multi-layered media but does not easily treat the field singularity existing at the edge of the conducting strip. Furthermore, the FEM is not efficient for the analysis

of open structures because it needs to treat the whole two-dimensional region. Contrary to the FEM, the BEM [6], [8], [11], [12] formulates an integral equation, not on the whole region, but only on the boundaries of dielectric substrates and on the surfaces of conductors. In addition, the BEM can handle the singularity existing at the edges of the conducting strip, and has no difficulty with open structure [6], [8]. In a structure with multi-layered media, however, formulating those integral equations on each boundary is complicated and time-consuming. This difficulty arises because of the use of a free-space Green's function in the BEM, which do not incorporate boundary conditions in the multi-layered media.

In this paper, we propose a new method of analysis which we call the partial-boundary element method (p-BEM). It is based on the quasi-TEM wave approximation, and its purpose is to carry out a more efficient and effective analysis of these transmission lines. This method introduces a concept of equivalent charge density [9] and uses the Green's function [7], [10] of a structure related to the original one, in which some dielectric region is replaced by other dielectric material. With this method, the boundary integral equations are formulated only on part of the boundaries, and therefore can avoid the above mentioned complication with the BEM. As applications of the p-BEM, we present an analysis of two kinds of striplines: (1) with a rectangular dielectric ridge and (2) with an embedded rectangular dielectric in three-layered media, as shown in Figs. 1 and 2.

II. The Partial-Boundary Element Method (p-BEM)

To describe the partial-boundary element method for the analysis of the structures shown in Figs. 1 and 2, we take up the structure of Fig. 1 as a model. It consists of a rectangular dielectric ridge with conducting strip on it, and a two-layer medium as substrate. The outer conductor is provided to correspond to the conductor shielded transmission line structure as well as for convenience of analysis. The dielectric materials involved are assumed lossless and isotropic, with electric parameters $\varepsilon_i (i = 1, 2, 3, 4)$. Strip and outer conductors are perfectly conducting. Physical dimensions are on the order of μm as are typical in transmission lines used in MMIC's [1], [2].

Because an inhomogeneous dielectric system does not support the TEM mode along the transmission line, hybrid modes are to be expected instead. To the structure shown in Fig. 1, however, the quasi-TEM wave approximation can still be effectively applied, since higher modes are difficult to excite when the widths of dielectric ridge and conducting strip are less than one half the operating microwave wavelength. For this reason, we shall in this paper develop the p-BEM under the quasi-TEM wave approximation [5], [8].

A. Principle of the p-BEM

Under the quasi-TEM wave approximation, the analysis of the transmission line structure consists in finding an electrostatic solution to a two-dimensional boundary-value problem. For the structure with a special cross-sectional analysis region shown in Fig. 1, the boundary integral equation (BIE) technique, for instance the BEM, is a suitable candidate for its flexibility to accommodate the arbitrary boundary. The BIE technique employs a Green's function, and boundary integral equations need to be formulated on boundaries where the Green's function does not satisfy their boundary conditions. Therefore, the BEM should treat all boundaries, including the boundaries of the dielectric ridge and the regular boundaries of the multi-layered media and outer conductor. This treatment is fairly complicated. On the other hand, if one can find a Green's function $G_0(\boldsymbol{\rho}|\boldsymbol{\rho}_0)$ which satisfies all boundary conditions in the structure, where $\boldsymbol{\rho}$ and $\boldsymbol{\rho}_0$ denote position vectors for observing point (x, y) and source point (x_0, y_0), then by replacing the strip conductor by a charge density distribution, the potential function $\phi(\boldsymbol{\rho})$ at any point in the cross-section can be obtained by a boundary integral given by [7]

$$\phi = \oint_{\Gamma_0} \sigma_0 G_0 \, d\Gamma, \tag{1}$$

where Γ_0 is an integral circumference around the surface of the strip conductor, and $\sigma_0(\boldsymbol{\rho}_0)$ is the charge density distribution on the surface. Once this integral expression of the potential is derived, the boundary integral equations can be easily formulated by following the procedure of the BIE technique. However, the difficulty in using (1) is to obtain the Green's function that satisfies all boundary conditions of the transmission line structure under consideration. For the structure shown in Fig. 1, it is obviously impractical because of the complexity of the boundary around the interface of the dielectric ridge, though the remaining boundaries are regular. For such a structure, it is advantageous to use the p-BEM, as presently described.

Consider the structure shown in Fig. 3, which is related to the original configuration shown in Fig. 1. This structure is defined by removing the rectangular cross-sectional dielectric ridge and the conducting strip. By setting up rectangular coordinates, and assuming that we have obtained the Green's function $G(\boldsymbol{\rho}|\boldsymbol{\rho}_0)$ which satisfies all boundary conditions in the structure shown in Fig. 3, we can then express the potential function $\phi(\boldsymbol{\rho})$ at any point in the cross-section of the original structure as

$$\phi = \oint_{\Gamma_0 + \Gamma_p} \sigma G \, d\Gamma, \tag{2}$$

where Γ_p is an integral circumference around the surface of the dielectric ridge and $\sigma(\boldsymbol{\rho}_0)$ is the equivalent charge density distribution on Γ_0 and Γ_p. The quantity σ is introduced and defined in Appendix. Equation (2) is the most important formula in this paper and its proof is given in detail in Appendix for a generalized two-dimensional boundary value problem. It should be noticed that the difference between the potential integral expressions in (1) and (2) is the addition of an integral around the interface of the dielectric ridge. Comparing with the conventional BEM, we need to treat only the "partial-boundary" instead of all boundaries in the structure under consideration. In this sense we call the integral expression of the potential in (2) a "partial-boundary integral" and name our method as "partial-boundary element method (p-BEM)". The procedure for the derivation of boundary integral equations

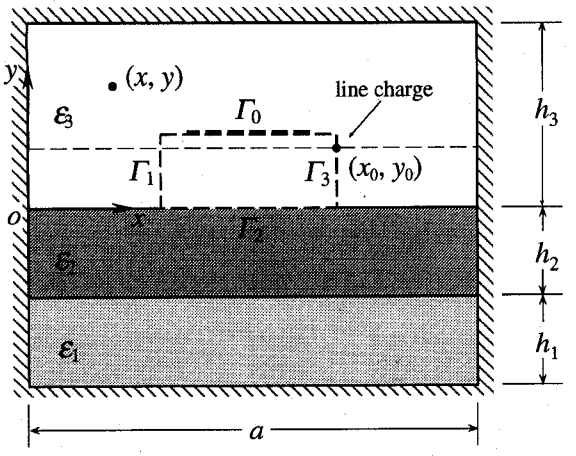

Fig. 3. Shielded structure with three dielectric layers.

from (2) is similar to that in the conventional BIE technique and is described in the following.

B. Green's Function in the Structure with Three-Layered Media

To formulate the boundary integral equations from the partial-boundary integral in (2), we must first find the Green's function. For the structure with multi-layered media as shown in Fig. 3, two techniques are usually employed to derive the Green's function. One is the image method, which uses single or multi infinite series of image charges to satisfy the boundary conditions on the interfaces of the layered media [7]. The other is the Fourier expanding or transformation technique in which a solution is obtained in the form of Fourier series or integral. In both cases, we can obtain the Green's function analytically. For the structure with the shielded conductor, the image charges are distributed in two-dimensional space and thus make the boundary integrals very complicated. In contrast, the Fourier expanding technique can be easily adapted to fit any number of layers. We use the Fourier expanding technique in the present paper. The Green's function in the third region which satisfies all boundary conditions in the structure shown in Fig. 3 is given by [10] where

$$\begin{aligned}\Delta_n(y) = {} & \varepsilon_2\varepsilon_2 \sinh\,\alpha_n h_1 \sinh\,\alpha_n h_2 \sinh\,\alpha_n y \\ & + \varepsilon_2\varepsilon_3 \sinh\,\alpha_n h_1 \cosh\,\alpha_n h_2 \cosh\,\alpha_n y \\ & + \varepsilon_3\varepsilon_1 \cosh\,\alpha_n h_1 \sinh\,\alpha_n h_2 \cosh\,\alpha_n y \\ & + \varepsilon_1\varepsilon_2 \cosh\,\alpha_n h_1 \cosh\,\alpha_n h_2 \sinh\,\alpha_n y \\ \alpha_n = {} & \frac{n\pi}{a}\end{aligned}$$

Here we assumed the line source is at (x_0, y_0) in the third region, too.

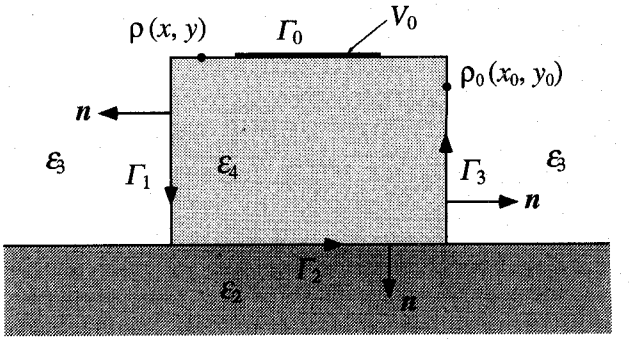

Fig. 4. Rectangular dielectric ridge and its boundaries.

C. Formulation of the Partial-Boundary Integral Equations

For convenience of derivation, we enlarge the part of the rectangular dielectric ridge and illustrate it again in Fig. 4. The boundary consists of one conductor surface Γ_0 to which a voltage V_0 is applied, and three dielectric interfaces denoted as $\Gamma_1, \Gamma_2, \Gamma_3$, respectively, and $\Gamma_p = \Gamma_1 + \Gamma_2 + \Gamma_3$. Moving the observing point to the boundaries, we obtain two kinds of boundary integral equations from (2) and the boundary conditions as follows.

On the perfectly conducting strip, we have

$$\oint_{\Gamma_0+\Gamma_p} \sigma G_{33}(\boldsymbol{\rho}|\boldsymbol{\rho}_0)\, d\Gamma = V_0, \quad \text{on } \Gamma_0, \tag{4.1}$$

and on the dielectric interfaces, we have

$$\begin{aligned}\varepsilon_3 \oint_{\Gamma_0+\Gamma_p} \sigma \frac{\partial G_{33}(\boldsymbol{\rho}^+|\boldsymbol{\rho}_0)}{\partial n}\, d\Gamma \\ = \varepsilon_4 \oint_{\Gamma_0+\Gamma_p} \sigma \frac{\partial G_{33}(\boldsymbol{\rho}^-|\boldsymbol{\rho}_0)}{\partial n}\, d\Gamma, \quad \text{on } \Gamma_1 \text{ and } \Gamma_3,\end{aligned} \tag{4.2}$$

$$\begin{aligned}\varepsilon_2 \oint_{\Gamma_0+\Gamma_p} \sigma \frac{\partial G_{23}(\boldsymbol{\rho}^+|\boldsymbol{\rho}_0)}{\partial n}\, d\Gamma \\ = \varepsilon_4 \oint_{\Gamma_0+\Gamma_p} \sigma \frac{\partial G_{33}(\boldsymbol{\rho}^-|\boldsymbol{\rho}_0)}{\partial n}\, d\Gamma, \quad \text{on } \Gamma_2.\end{aligned} \tag{4.3}$$

where G_{23} is a Green's function in region 2 created by the source in region 3, and satisfies following boundary equation:

$$-\varepsilon_2 \frac{\partial G_{23}(\boldsymbol{\rho}^+|\boldsymbol{\rho}_0)}{\partial n} + \varepsilon_3 \frac{\partial G_{33}(\boldsymbol{\rho}^-|\boldsymbol{\rho}_0)}{\partial n} = \delta(\boldsymbol{\rho} - \boldsymbol{\rho}_0) \quad \text{on } \Gamma_2. \tag{5}$$

The quantities $\boldsymbol{\rho}^+$ and $\boldsymbol{\rho}^-$ denote the position vectors of the observing point infinitely close to the position $\boldsymbol{\rho}$ on the boundary Γ_p but slightly outside (+ sign) and inside (− sign) the dielectric region 4, respectively.

$$G_{33} = \sum_{n=1}^{\infty} \frac{2}{n\pi\varepsilon_3} \begin{cases} \dfrac{\Delta_n(y) \sinh\,\alpha_n(h_3 - y_0)}{\Delta_n(h_3)} \cdot \sin\,\alpha_n x_0 \sin\,\alpha_n x, & 0 \le y \le y_0, 0 \le x \le a \\ \dfrac{\Delta_n(y_0) \sinh\,\alpha_n(h_3 - y)}{\Delta_n(h_3)} \cdot \sin\,\alpha_n x_0 \sin\,\alpha_n x, & y_0 \le y \le h_3, 0 \le x \le a \end{cases} \tag{3}$$

D. Treatment of the Singularity of Green's Function in the Boundary Integrals

Before calculating the integrals in the above equations numerically on a computer, we have to treat the singularity in the Green's function in (4.2) and (4.3) since the singularity can lead to a serious computation error. Referring to Fig. 4, the Green's function, denoted as G_p, which satisfies the boundary conditions can be rewritten as a logarithmic function when the observing point is close enough to the source point, and is given as

$$G_p(\boldsymbol{\rho}|\boldsymbol{\rho}_0) = \frac{1}{2\pi\varepsilon_p} \ln|\boldsymbol{\rho} - \boldsymbol{\rho}_0|, \quad \text{when } |\boldsymbol{\rho} - \boldsymbol{\rho}_0| \to 0, \quad (6.1)$$

where

$$\varepsilon_p = \begin{cases} \varepsilon_3, & \text{on } \Gamma_1 \text{ and } \Gamma_3 \\ (\varepsilon_2 + \varepsilon_3)/2, & \text{on } \Gamma_2 \end{cases}, \quad (6.2)$$

and

$$|\boldsymbol{\rho} - \boldsymbol{\rho}_0| = \sqrt{(x - x_0)^2 + (y - y_0)^2}.$$

The integral of the normal derivative of the function $-(1/2\pi)\ln|\boldsymbol{\rho} - \boldsymbol{\rho}_0|$ over an infinitesimal smooth boundary integral region where $|\boldsymbol{\rho} - \boldsymbol{\rho}_0| \to 0$ gives a finite value $-1/2$ for the outside observing point $\boldsymbol{\rho}^+$ and $+1/2$ for the inside point $\boldsymbol{\rho}^-$. Applying this treatment into (4.2) and (4.3), and substituting (5) to (4.3), we can rewrite the integrals after extracting the singularity part as follows:

$$\frac{\varepsilon_4 + \varepsilon_3}{2\varepsilon_3}\sigma + (\varepsilon_4 - \varepsilon_3) \oint_{\Gamma_0 + \Gamma_p \not\subset (x,y)} \sigma \frac{\partial G_{33}}{\partial n}\, d\Gamma = 0, \quad \text{on } \Gamma_1 \text{ and } \Gamma_3, \quad (7.1)$$

$$\frac{\varepsilon_4 + \varepsilon_2}{\varepsilon_3 + \varepsilon_2}\sigma + (\varepsilon_4 - \varepsilon_2) \oint_{\Gamma_0 + \Gamma_p \not\subset (x,y)} \sigma \frac{\partial G_{33}}{\partial n}\, d\Gamma = 0, \quad \text{on } \Gamma_2, \quad (7.2)$$

where position vectors slightly outside and inside region 4 coalesce into the position vector on the boundary Γ_p, and are omitted for simplicity. On the other hand, the singularity in (4.1) needs not be treated since the integral of the logarithmic function in (6) over a infinitely small integral region vanishes, so that it will not lead to a significant error in computation.

E. Boundary Discretization of the Partial-Boundary Integral Equations

After the singular parts having been removed, the partial-boundary integral (4.1), (7.1), and (7.2) can be solved by boundary discretization as usually done in the BEM [6], [8]–[10]. By setting up a local coordinate ξ along the boundary, we can express the equivalent boundary charge density distribution σ as

$$\sigma = \sum_{i=1}^{m} \sigma_i f_i(\xi) \quad (8)$$

where m is the total number of the boundary elements, and $f_i(\xi)$is an interpolating function on the ith boundary element. The most simple interpolating function $f_i(\xi)$ is the step function defined by

$$f_i(\xi) = \begin{cases} 1, & \text{on the } i\text{th element} \\ 0, & \text{elsewise.} \end{cases} \quad (9)$$

Substituting (8) and (9) into the partial-boundary integral (4), we get a series of simultaneous equations for σ_i as

$$\boldsymbol{H} \cdot \boldsymbol{\sigma} = \boldsymbol{V} \quad (10.1)$$

$$\boldsymbol{\sigma} = (\sigma_1, \sigma_2, \cdots, \sigma_m)^T \quad (10.2)$$

$$\boldsymbol{V} = \underbrace{(V_0, V_0, \cdots, V_0}_{m_0}, \underbrace{0, \cdots, 0)^T}_{m_p} \quad (10.3)$$

where $m = m_0 + m_p$, m_0 is the number of boundary elements on the strip conductor, m_p is the number of boundary elements on dielectric interfaces, and $\boldsymbol{H}$ is a coefficient matrix associated with the Green's function and the boundary integral equations on each element.

After finding the equivalent boundary charge density distribution σ by solving the simultaneous (10) on a computer, we can easily obtain the true charge density distribution as discussed in the Appendix. The transmission line characteristics can then be calculated through the line capacitance per unit length, which is the integral of the charge density distribution over the surface of the strip conductor [5], [9], [10].

III. Numerical Results for Two Striplines

As an illustration of the p-BEM, we present two sets of numerical results for the two striplines shown in Figs. 1 and 2.

First we analyze the stripline with a rectangular dielectric ridge in three-layered media. The associated geometrical and dielectric parameters are as follows: $a/b = 2.0$, $h_1/b = 0.4$, $h_2/b = 0.2$, $h_3/b = 0.4$, $\varepsilon_1 = 1.0$, $\varepsilon_2 = 10.0$, $\varepsilon_3 = 1.0$.

To verify the accuracy of the numerical results, the convergence of the characteristic impedance and the effective dielectric constant versus both the number of Fourier terms N for the Green's function in (3), shown at the bottom of the previous page, and the number of the elements m_0 on the strip conductor, is investigated first. The numerical results of the convergence are shown in Fig. 5(a) and (b). These results demonstrate that to get a relative error less than 1% in both the characteristic impedance and the effective dielectric constant, the number of Fourier terms N must be greater than about 3000, and the number of elements on the strip conductor $m_0 > 15$. All numerical results shown subsequently in this paper are calculated with $N = 4000$ and $m_0 = 20$ or more. The number of elements on the dielectric interface is set at $m_p = 30$ or more.

Fig. 6 shows the characteristic impedance and the effective dielectric constant versus the normalized width d/b of the dielectric ridge with dielectric constant ε_4 as parameter.

Fig. 7(a) and (b) show the characteristic impedance and the effective dielectric constant versus the normalized height h/b of the dielectric ridge, with the normalized width w/b of strip conductor as parameter.

Next we analyze the stripline with an embedded rectangular dielectric in three-layered media. The associated geometrical

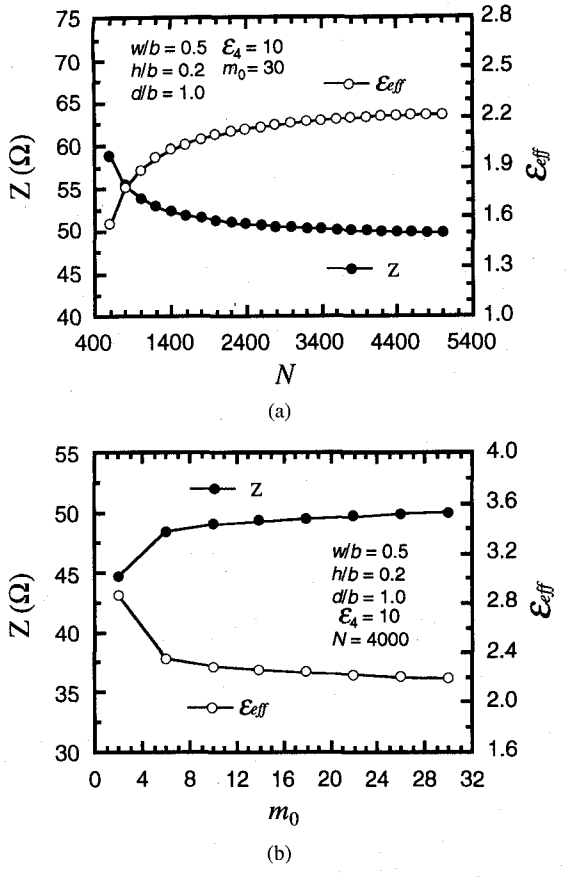

Fig. 5. Convergence of numerical results for characteristic impedance and effective dielectric constant versus (a) the number of Fourier terms N and (b) the number of elements on strip conductor m_0.

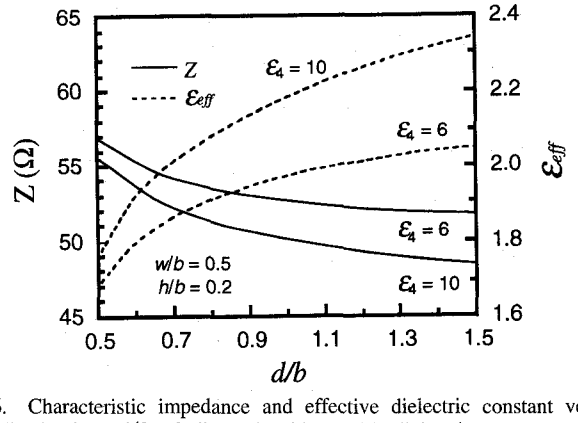

Fig. 6. Characteristic impedance and effective dielectric constant versus normalized width d/b of dielectric ridge, with dielectric constant ε_4 as parameter.

and dielectric parameters are as follows:$a/b = 2.0$, $h_1/b = 0.2$, $h_2/b = 0.4$, $h_3/b = 0.4$, $\varepsilon_1 = 1.0$, $\varepsilon_2 = 10.0$, $\varepsilon_3 = 1.0$.

Fig. 8 shows the normalized charge density distribution on the strip. For the case $w < d$, a relatively small dielectric constant $\varepsilon_4 < \varepsilon_2$ gives a weak charge density on the strip, while for the case of $w > d$, a relatively large $\varepsilon_4 > \varepsilon_2$ gives the same result. Therefore, the charge density on the strip conductor can be controlled by the embedded dielectric constant ε_4. A weak charge density associates with low loss of the stripline.

Fig. 9(a) and (b) show the characteristic impedance and the effective dielectric constant versus the normalized width

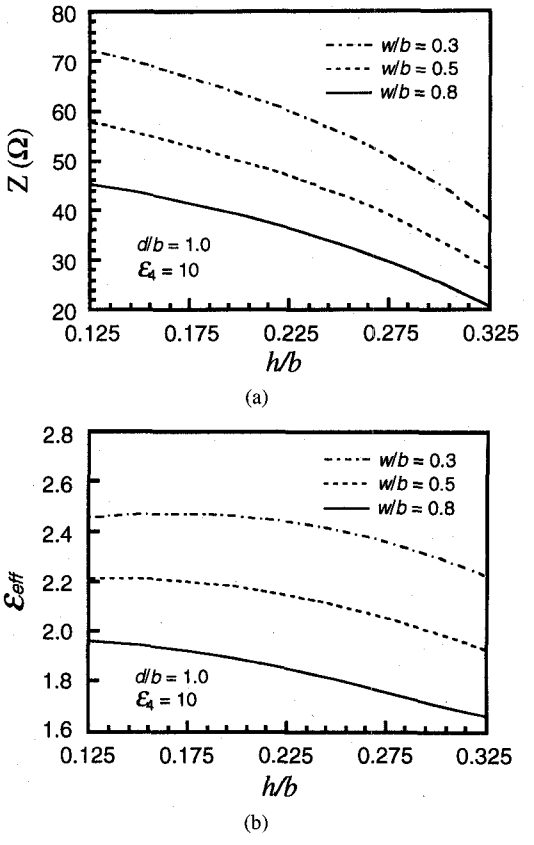

Fig. 7. (a) Characteristic impedance and (b) effective dielectric constant versus normalized height h/b of dielectric ridge, with normalized width w/b of strip conductor as parameter.

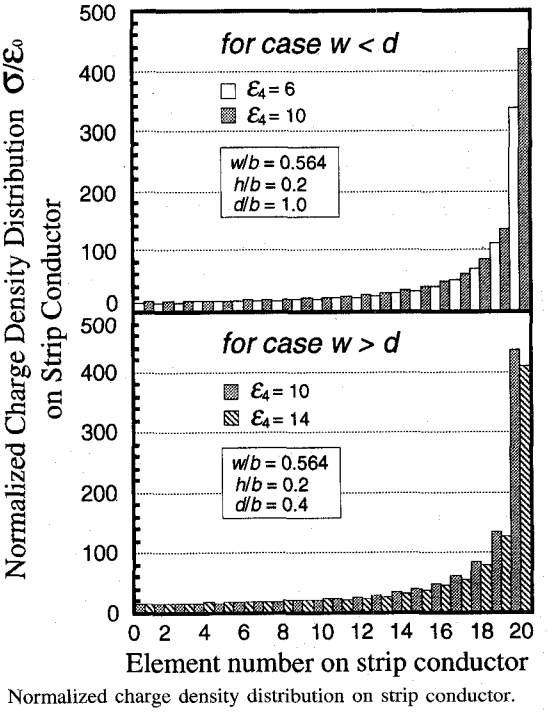

Fig. 8. Normalized charge density distribution on strip conductor.

d/b of the embedded dielectric, with dielectric constant ε_4 as parameter. These results demonstrate that either when $w < d$, or when $w > d$, the characteristics are almost flat, while for d close to w, the characteristics vary sharply. This is due

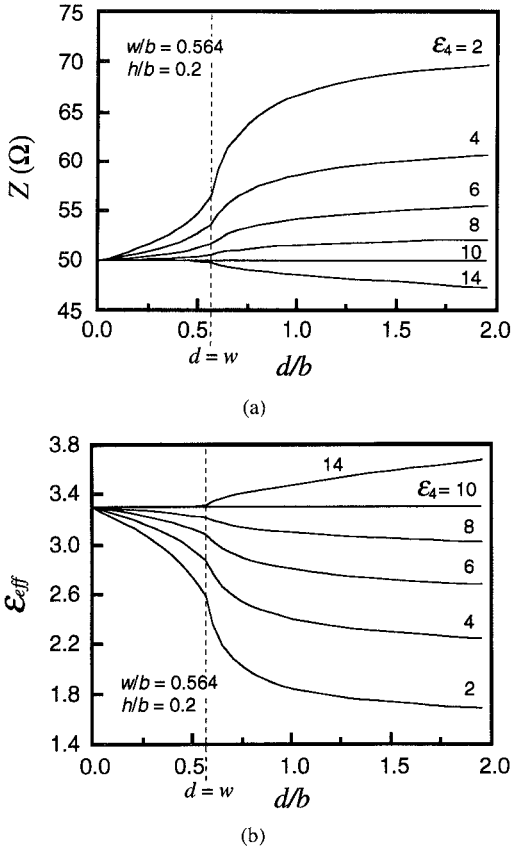

Fig. 9. (a) Characteristic impedance and (b) effective dielectric constant versus normalized width d/b of embedded dielectric, with dielectric constant ε_4 as parameter.

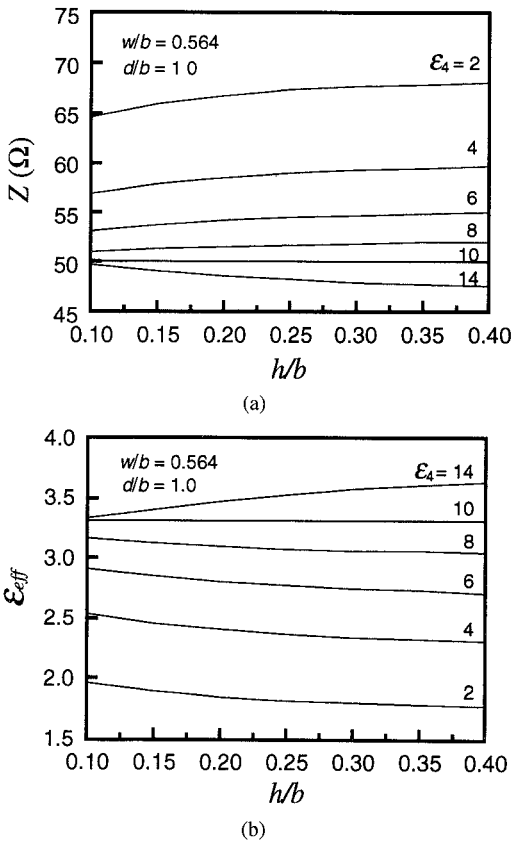

Fig. 10. (a) Characteristic impedance and (b) effective dielectric constant versus normalized depth h/b of embedded dielectric, with dielectric constant ε_4 as parameter.

to the fact that when d approaches w, the presence of the embedded dielectric strongly affects the charge density on the strip conductor.

Fig. 10(a) and (b) show the characteristic impedance and the effective dielectric constant versus the normalized depth h/b of the embedded dielectric with dielectric constant ε_4 as parameter.

It took about 10 seconds of CPU time to calculate one set of the characteristic data on a workstation SUN SPARCstation 2.

IV. Discussions on p-BEM

It should be noted that the formulation of the boundary integral equations in Section II does not require that the dielectric ridge be rectangular, though we used the rectangular structure as a model. Indeed, we have proved the partial-boundary integral for a general configuration in the Appendix, so the formulation can be applied to an arbitrary cross-sectional dielectric ridge, and the p-BEM can be employed for the analysis of such structure.

As an extension to the boundary integral equation (BIE) technique, the p-BEM provides a mean of formulating the BIE's and selecting the Green's function. The discretization of the formulated BIEs is done in a similar fashion as with the BEM. The p-BEM can also be considered as an extension of the BEM from the point of view of introducing the concept of the equivalent charge density and using the Green's function of a structure related to the original one. The most important merit of the p-BEM is that it provides a straight forward and optimum approach to formulate the BIE's in a boundary value problem, the BIE's being formulated only on the partial-boundaries. This point is particularly useful in the analysis of striplines with arbitrary cross-sectional dielectric in multi-layered media. The comparison between the p-BEM and the BEM is given in Table I.

V. Conclusion

In this paper, a new method of analysis called the partial-boundary element method (p-BEM), has been proposed for the analysis of striplines with arbitrary cross-sectional dielectric in multi-layered media. In the p-BEM, the boundary integral equations can be formulated only on the surfaces of the strip conductor(s) and the boundaries of the arbitrary cross-sectional dielectric. The merit of this method is that the number of boundaries to treat is small compared with the conventional boundary integral equation methods such as the BEM in which the Green's function in free space is usually employed. Striplines: (1) with a rectangular dielectric ridge and (2) with an embedded rectangular dielectric in multi-layered media are characterized in this paper as applications of the p-BEM. The numerical results present many significant aspects of these lines, and show the effectiveness of the p-BEM.

TABLE I
COMPARISON BETWEEN BEM AND p-BEM

Comparison Term	BEM[6]	p-BEM
Green's function used in formulation	Green's function in free-space	Green's function satisfying partial-boundary conditions
degree of difficulty to obtain Green's function	easy	comparatively complicated
boundaries to be treated	all	part
formulation of boundary integral equations	complicated	straight forward
boundary variables used in formulation	potential, boundary charge density or both	equivalent boundary density distribution only
boundary discretization	using interpolate function	using interpolate function
treatment of singularity	necessary	necessary
applicability to boundary value problem	wide	comparatively wide
applicability to multi-media (i.e. multi-boundaries) problem	complicated	simple (by selecting an appropriate Green's function)
extension to 3-dimensional problem	possible and easy	possible and easy
extension to full wave analysis	possible and comparatively easy	possible but may be difficult
strong point	applicable to all problems with one Green's function	formulation only on partial-boundary
weak point	complicated for multi-media problem	have to find a specific Green's function for a specific problem
identity of p-BEM	when selecting Green's function in free-space, the p-BEM is similar to the indirect BEM, but builds up the boundary integral equations in a more straight forward way.	

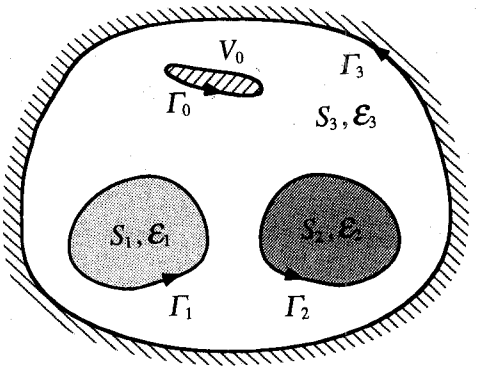

Fig. A-1. Two-dimensional boundary problem of static electric field in three dielectric regions.

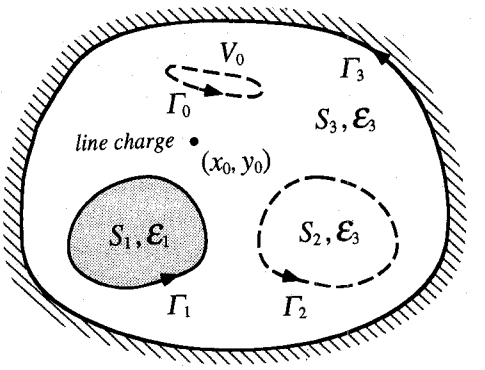

Fig. A-2. An associated two-dimensional boundary problem of static electric field, with ε_2 replaced by ε_3.

APPENDIX
DERIVATION OF THE PARTIAL-BOUNDARY INTEGRAL

Consider a two-dimensional static electric boundary value problem as shown in Fig. A-1. The problem consists of one inner conductor with an applied voltage V_0 and three dielectric regions with electric parameters $\varepsilon_i (i = 1, 2, 3)$ surrounded by shield conductor as seen in Fig. A-1. The inner conductor is denoted by a closed curve Γ_0, and the three regions are denoted $S_i (i = 1, 2, 3)$, surrounded respectively by three closed curves $\Gamma_i (i = 1, 2, 3)$ in the xy plane, respectively. The dielectric materials involved in this structure are assumed lossless and isotropic, and the inner and outer conductors are perfectly conducting.

Denoting the potentials for the static electric field in the three regions by $\phi_i(x, y)$ (i = 1, 2, 3), we have Laplace's equation as follows:

$$\nabla^2 \phi_i(x, y) = 0, \qquad (x, y) \in S_i, \qquad i = 1, 2, 3, \tag{A.1}$$

where $\nabla^2 = \partial^2/\partial x^2 + \partial^2/\partial y^2$.

To solve for the potentials in each region, the boundary integral equation technique is useful but a Green's function that satisfies all boundary conditions in the structure in Fig. A-1 is difficult to find. To avoid the difficulty, let us consider another Green's function that satisfies all boundary conditions not in the structure in Fig. A-1 but in a structure related to it as shown in Fig. A-2. We assume that this Green's function is easier to find than the original one. The relevant structure, as illustrated in Fig. A-2, is made up by replacing the ε_2 dielectric regions S_2 with ε_3 dielectric region, and removing the inner conductor in Fig. A-1.

In Fig. A-2, assuming that the Green's functions due to a line charge located at an arbitrary point (x_0, y_0) in the region S_2 or S_3 is denoted as $G_{13}(x, y)$ in region S_1 and $G_{33}(x, y)$ in region S_2 and S_3, respectively, then we have

$$\nabla^2 G_{13}(x, y|x_0, y_0) = 0, \qquad (x, y) \in S_1, \tag{A.2}$$

$$\nabla^2 G_{33}(x, y|x_0, y_0) = -\frac{1}{\varepsilon_3}\delta(x - x_0, y - y_0), \qquad (x, y) \in S_3 \text{ or } S_2. \tag{A.3}$$

These Green's functions G_{13} and G_{33} are assumed to satisfy all boundary conditions in the relevant structure in Fig. A-2. Thus we have the following boundary conditions for the potential functions $\phi_1(x, y), \phi_2(x, y)$ and $\phi_3(x, y)$ and the Green's functions G_{13} and G_{33}:

$$\phi_3 = V_0, \quad \text{on } \Gamma_0, \tag{A.4.1}$$

$$\phi_1 = \phi_3, \quad \varepsilon_1 \frac{\partial \phi_1}{\partial n} = \varepsilon_3 \frac{\partial \phi_3}{\partial n}, \quad \text{on } \Gamma_1, \tag{A.4.2}$$

$$\phi_2 = \phi_3, \quad \varepsilon_3 \frac{\partial \phi_2}{\partial n} = \varepsilon_3 \frac{\partial \phi_3}{\partial n}, \quad \text{on } \Gamma_2, \tag{A.4.3}$$

$$\phi_3 = 0, \quad \text{on } \Gamma_3, \tag{A.4.4}$$

and

$$G_{13} = G_{33}, \quad \varepsilon_1 \frac{\partial G_{13}}{\partial n} = \varepsilon_3 \frac{\partial G_{33}}{\partial n}, \quad \text{on } \Gamma_1, \tag{A.5.1}$$

$$G_{33} = 0, \quad \text{on } \Gamma_3. \tag{A.5.2}$$

Applying Green's second integral theorem

$$\iint_S (\phi\nabla^2 G - G\nabla^2\phi)\, ds = \oint_\Gamma \left(\phi\frac{\partial G}{\partial n} - G\frac{\partial\phi}{\partial n}\right) d\Gamma \quad \text{(A.6)}$$

to region S_1, we have

$$\iint_{S_1} (\phi_1\nabla^2 G_{13} - G_{13}\nabla^2\phi_1)\, ds_1 = \oint_{\Gamma_1} \left(\phi_1\frac{\partial G_{13}}{\partial n} - G_{13}\frac{\partial\phi_1}{\partial n}\right) d\Gamma. \quad \text{(A.7)}$$

Substituting (A.1) and (A.2) into this equation gives

$$-\varepsilon_1 \oint_{\Gamma_1} \left(\phi_1\frac{\partial G_{13}}{\partial n} - G_{13}\frac{\partial\phi_1}{\partial n}\right) d\Gamma = 0. \quad \text{(A.8)}$$

Working similar way with region S_2, we have

$$\iint_{S_2} (\phi_2\nabla^2 G_{33} - G_{33}\nabla^2\phi_2)\, ds = \iint_{\Gamma_2} \left(\phi_2\frac{\partial G_{33}}{\partial n} - G_{33}\frac{\partial\phi_2}{\partial n}\right) d\Gamma \quad \text{(A.9)}$$

and substituting (A.1) and (A.3) into this equation gives

$$-\varepsilon_3 \oint_{\Gamma_2} \left(\phi_2\frac{\partial G_{33}}{\partial n} - G_{33}\frac{\partial\phi_2}{\partial n}\right) d\Gamma = \begin{cases} \phi_2, & (x_0, y_0) \in S_2 \\ 0, & (x_0, y_0) \notin S_2 \end{cases}. \quad \text{(A.10)}$$

In region S_3, we have

$$\iint_{S_3} (\phi_3\nabla^2 G_{33} - G_{33}\nabla^2\phi_3)\, ds = \oint_{\Gamma_3'} \left(\phi_3\frac{\partial G_{33}}{\partial n} - G_{33}\frac{\partial\phi_3}{\partial n}\right) d\Gamma, \quad \text{(A.11)}$$

where $\Gamma_3' = \Gamma_3 - \Gamma_1 - \Gamma_2 - \Gamma_0$. Expanding the right-hand term of this equation as

$$\oint_{\Gamma_3'} = \oint_{\Gamma_3} - \oint_{\Gamma_1} - \oint_{\Gamma_2} - \oint_{\Gamma_0} \quad \text{(A.12)}$$

and substituting (A.4), (A.5) and (A.8) into (A.12) gives

$$\oint_{\Gamma_2} = 0, \qquad \oint_{\Gamma_1} = 0, \quad \text{(A.13)}$$

and

$$\oint_{\Gamma_0} \phi_3\frac{\partial G_{33}}{\partial n}\, d\Gamma = V_0 \oint_{\Gamma_0} \frac{\partial G_{33}}{\partial n}\, d\Gamma = 0 \quad \text{(A.14)}$$

because no net electric flux remains in the region enclosed by Γ_0.

Therefore (A.11) can be rewritten as

$$-\varepsilon_3 \oint_{\Gamma_0} G_{33}\frac{\partial\phi_3}{\partial n}\, d\Gamma + \varepsilon_3 \oint_{\Gamma_2} \left(\phi_3\frac{\partial G_{33}}{\partial n} - G_{33}\frac{\partial\phi_3}{\partial n}\right) d\Gamma = \begin{cases} \phi_3, & (x_0, y_0) \in S_3 \\ 0, & (x_0, y_0) \notin S_3 \end{cases}. \quad \text{(A.15)}$$

Combining (A.10) and (A.15) in regions S_2 and S_3, respectively, we have

$$\phi_2 = \oint_{\Gamma_0} G_{33}\left(-\varepsilon_3\frac{\partial\phi_3}{\partial n}\right) d\Gamma + \oint_{\Gamma_2} G_{33}\left(\varepsilon_3\frac{\partial\phi_2}{\partial n} - \varepsilon_3\frac{\partial\phi_3}{\partial n}\right) d\Gamma, \quad \text{(A.16)}$$

$$\phi_3 = \oint_{\Gamma_0} G_{33}\left(-\varepsilon_3\frac{\partial\phi_3}{\partial n}\right) d\Gamma + \oint_{\Gamma_2} G_{33}\left(\varepsilon_3\frac{\partial\phi_3}{\partial n} - \varepsilon_3\frac{\partial\phi_3}{\partial n}\right) d\Gamma. \quad \text{(A.17)}$$

Defining σ as

$$\sigma = \begin{cases} -\varepsilon_3\dfrac{\partial\phi_3}{\partial n}, & \text{on } \Gamma_0 \\ \varepsilon_3\dfrac{\partial\phi_2}{\partial n} - \varepsilon_3\dfrac{\partial\phi_3}{\partial n}, & \text{on } \Gamma_2 \end{cases}, \quad \text{(A.18)}$$

we can then express the potentials in regions S_2 and S_3 simply as follows:

$$\phi_{2,3} = \oint_{\Gamma_0+\Gamma_2} \sigma G_{33}\, d\Gamma. \quad \text{(A.19)}$$

On the other hand, to find the potential function in region S_1, the line charge (x_0, y_0) must be moved into the region. When the source is at (x_0, y_0) in region S_1, we have

$$\nabla^2 G_{11}(x, y|x_0, y_0) = -\frac{1}{\varepsilon_1}\delta(x - x_0, y - y_0), \quad (x, y) \in S_1, \quad \text{(A.20)}$$

$$\nabla^2 G_{31}(x, y|x_0, y_0) = 0, \quad (x, y) \in S_3. \quad \text{(A.21)}$$

Applying Green's second integral theorem to the region S_1 and using the boundary conditions for G_{11} and G_{31} as shown in (A.5) for G_{13} and G_{33}, and following the procedures used previously to the region S_3, we can get

$$\phi_1 = \oint_{\Gamma_0} G_{31}\left(-\varepsilon_3\frac{\partial\phi_3}{\partial n}\right) d\Gamma + \oint_{\Gamma_2} G_{31}\left(\varepsilon_3\frac{\partial\phi_2}{\partial n} - \varepsilon_3\frac{\partial\phi_3}{\partial n}\right) d\Gamma. \quad \text{(A.22)}$$

We have

$$G_{31} = G_{13}, \quad \text{(A.23)}$$

from the symmetry of Green's functions between the source point (x_0, y_0) and the observing point (x, y). Using the variable σ defined in (A.18), the potential in region S_1 can then be expressed as

$$\phi_1 = \oint_{\Gamma_0+\Gamma_2} \sigma G_{13}\, d\Gamma. \quad \text{(A.24)}$$

Now by putting together the integrals in (A.19) and (A.24), we can express the potential in each region in the two-dimensional problem in Fig. A-1 in a unified way as

$$\phi = \oint_{\Gamma_0+\Gamma_2} \sigma G\, d\Gamma. \quad \text{(A.25)}$$

This integral for potentials is called the "partial-boundary integral" in this paper, in contrast to the conventional boundary

integral equation in which the integrals for the potential must be taken over all boundaries in Fig. A-1.

The variable σ defined in (A.18) has units of charge density. In some cases, it is just the true charge density. In general, however, σ is an equivalent charge density distribution on the partial-boundary without physical significance and just defined as in (A.18). The true charge density on the conductor surface Γ_0 can be obtained by simply multiplying σ with a constant associated with the dielectric constants.

We note that by following the above procedure, the partial-boundary integral in (A.25) can easily be obtained for more dielectric regions than in Fig. A-1. For example, we can divide region 1 into two regions, provided the Green's function used in (A.25) satisfies the corresponding additional boundary conditions.

ACKNOWLEDGMENT

The authors are very much thankful for the helpful discussions with Professor E. Yamashita, the University of Electro-Communications.

REFERENCES

[1] T. Tokumitsu, T. Hiraoka, H. Nakano, and M. Arake, "Multilayers MMIC using a 3 μm $\times$3 μm-layer dielectric film structure," in *IEEE MTT-S Int. Microwave Symp. Dig.*, 1990, pp. 831–834.

[2] H. J. Finlay, R. H. Jansen, J. A. Jenkins, and I. G. Eddison, "Accurate characterization and modeling of transmission lines for GaAs MMIC's," *IEEE Trans. Microwave Theory Tech.*, vol. MTT-36, no. 6, pp. 961–967, June 1988.

[3] H. B. Sequeira, J. A. McClintock, B, Young, and T. Itoh, "A millimeter-wave Microslab^{TM} Oscillator," *IEEE Trans. Microwave Theory Tech.*, vol. 34, no. 12, pp. 1333–1336, Dec. 1989.

[4] T. Itoh, "Generalized spectral domain method for multiconductor printed lines and its application to turnable suspended microstrip," *IEEE Trans. Microwave Theory Tech.*, vol. 26, no. 12, pp. 983–987, Dec. 1978.

[5] E. Yamashita, K. R. Li, and Y. Suzuki, "Characterization method and simple design formulas of MSC lines proposed for MMIC's," *IEEE Trans. Microwave Theory Tech.*, vol. MTT-35, pp. 1355–1362, 1987.

[6] C. A. Brebbia, *The Boundary Element Method for Engineers*. London: Petch, 1978.

[7] R. E. Collin, *Field Theory of Guided Waves*, 2nd ed. New York: IEEE Press, 1991, ch. 2.

[8] K. R. Li and Y. Fujii, "Indirect boundary element method applied to generalized microstripline analysis with application to side-proximity effect in MMIC," *IEEE Trans. Microwave Theory Tech.*, vol. MTT-40, no. 2, pp. 237–244, Feb. 1992.

[9] C. E. Smith and R.-S. Chang, "Microstrip transmission line with finite-width dielectric," *IEEE Trans. Microwave Theory Tech.*, vol. MTT-28, no. 2, pp. 90–94, Feb. 1980.

[10] E. Yamashita and K. Atsuki, "Analysis of thick-strip transmission lines," *IEEE Trans. Microwave Theory Tech.*, vol. MTT-19, no. 1, pp. 120–122, Jan. 1971.

[11] S. Schroeder and I. Wolff, "A new hybrid mode boundary integral method for analysis of MMIC waveguides with complicated cross-section," in *IEEE MTT-S Int. Microwave Symp. Dig.*, 1989, pp. 711–714.

[12] T. N. Chang and C. H. Tan, "Analysis of a shielded microstrip line with finite metallization thickness by the boundary element method," *IEEE Trans. Microwave Theory Tech.*, vol. MTT-38, no. 8, pp. 1130–1132, Aug. 1990.

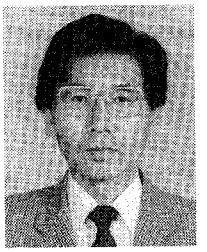

Kazuhiko Atsuki (M'89) was born in Tokyo, Japan, on November 2, 1942. He received the B.Eng. and M.Eng. degrees from the University of Electro-communications, Tokyo, Japan, and the Dr.Eng. degree from the University of Tokyo, Tokyo, Japan, all in electrical engineering, in 1965, 1967, and 1979, respectively.

He became a research assistant in 1967, an associate professor in 1982, and a professor in 1990 in the Department of Electronics, the University of Electro-communications, Tokyo, Japan. Presently his research deals with electromagnetic theory, microwave and optical waveguides, and its applications.

Dr. Atsuki is a member of the Institute of Electronics, Information and Communication Engineers (IEICE) of Japan and the Institute of Electrical Engineers of Japan.

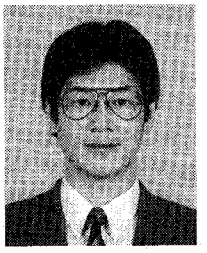

Keren Li (M'93) was born in Jiangsu Province, China, on June 22, 1963. He received the B.Eng. degree from the Nanjing Institute of Technology (now Southeast University), Nanjing, China, in July 1983, the M.Eng. degree from the University of Electro-communications, Tokyo, Japan, in March 1987, both in electronic engineering, and the Ph.D. degree in optical communications from the University of Tokyo, Tokyo, Japan, in March 1991.

He became a research associate of the University of Electro-communications in April 1991 and lecturer in April 1994. His research interests include electromagnetic analysis, microwave circuits, optical waveguides and optical devices in high speed optical communications, and the interactions between microwaves and optic waves.

Dr. Li is a member of the Institute of Electronics, Information and Communication Engineers (IEICE) of Japan.